Proceedings of the 2013 21st International Conference on Nuclear Engineering
ICONE21
July 29 - August 2, 2013, Chengdu, China

ICONE21-16342

ELECTROMAGNETIC SELF-LOCKING DEVICE FOR AIR CYLINDERS IN SPENT FUEL STORAGE SYSTEM OF PEBBLE-BED HIGH TEMPERATURE GAS-COOLED REACTOR

Bin Wu
Institute of Nuclear and New Energy Technology,
Tsinghua University
Beijing, CHINA

Jinhua Wang
Institute of Nuclear and New Energy Technology,
Tsinghua University
Beijing, CHINA

Yue Li
Institute of Nuclear and New Energy Technology,
Tsinghua University
Beijing, CHINA

Jiguo Liu
Institute of Nuclear and New Energy Technology,
Tsinghua University
Beijing, CHINA

ABSTRACT

In the spent fuel storage system of pebble-bed high temperature gas-cooled reactor, several air cylinders would be employed in complex machines, such as the spent fuel charging apparatus and the spent fuel canister crane. The cylinders were designed to actuate movements smoothly in radioactive environment. In order to lock them in safe position when the compressed air source is offline by accident, an electromagnetic self-locking device was designed. When power-off, the compressive spring would push out the lock plunger to enable self-lock. When power-on, the lock plunger would be withdrawn by the magnetic force of the coil to unlock the cylinder. In order to optimize the design more efficiently, numerical simulation was performed to optimize geometry parameters of the structure surrounding the working air gap so as to improve the performance of the device. A prototype was then fabricated. Combining the simulation results with experimental test, the actuating force characteristics of the device in locking and unlocking process was analyzed. The temperature rise when the device stays unlocked with power supply was also calculated and validated. The results showed that this electromagnetic self-locking device could realize the locking and unlocking functions effectively, and the maximum temperature rise also conforms the required limit. The as-fabricated device would help guarantee the fail-safe feature of the air cylinders of complex machines in compressed air outage.

INTRODUCTION

Many electric, magnetic and pneumatic components would be utilized to handle spherical fuel elements in pebble-bed high temperature gas-cooled reactor [1-2]. In the spent fuel storage system, several air cylinders would be employed in complex machines, such as the spent fuel charging apparatus and the spent fuel canister crane. These oil-free pneumatic cylinders were designed to actuate movements smoothly in radioactive environment. In case the compressed air source were offline by accident, however, the piston might slide away to unexpected position. In order to keep it in safe position, a self-locking device would be needed.

In this paper, an electromagnetic self-locking device was designed for a pneumatic cylinder in spent fuel storage system. Its working pressure was 0.5 MPa(G). It could be installed on the side wall of the cylinder with a plunger inserted through the wall into the cylinder. When power-off, the compressive spring would push out the lock plunger to enable self-lock. When power-on in normal situation, the lock plunger would be drawn out of the cylinder by magnetic attraction to disable self-lock.

Detailed structure of the device must be optimized to improve its performance. As a kind of numerical simulation method, finite element analysis software ANSYS was employed to calculate and optimize the design efficiently [3]. Simulation was performed to investigate the influence of some critical geometry parameters on magnetic field. The simulation results showed that optimized design could obtain adequate attracting and pushing forces. Besides, temperature field distribution was also simulated to verify that the temperature rise was in safe range. Moreover,

A prototype of self-locking device was fabricated. The experimental results of the prototype met the design requirements and validated the simulation results.

PROTOTYPE DESIGN

Materials

The following materials were utilized in the self-locking device (summarized in Table 1). Soft magnetic alloy 1JN (GB/T 14986-2008) and martensitic stainless steel 14Cr17Ni2 (S43110) were employed to manufacture the parts located in the magnetic circuit, including the magnetic plate, stationary core, movable core, tubular support and the coil shell. These magnetic materials were used to reduce reluctance out of the working air gap. The non-magnetic tube section and the isolation ring were made of austenitic stainless steel. Other structural parts were also made of austenitic stainless steel, such as signal pole and guide sleeve. This device can be entirely made of irradiation resistant materials to ensure its use in a radioactive environment. Typically it could tolerate a considerable accumulated dose of 1×10^7 rad.

Table 1 Parts of self-locking device and their material property

Part name	Material	Relative magnetic permeability
signal pole, guide sleeve, non-magnetic tube section, isolation ring	Austenitic stainless steel	1.01
coil shell, tubular support, stationary core	Martensitic stainless steel	Non-linear
magnetic plate, movable core	Soft magnetic alloy	Non-linear
Rubber mat	Rubber	1.01
Coil framework	Polyimide	1.01
Copper sheet	Copper	1.01
-	Air	1

Design

A typical structure of the self-locking device was demonstrated in Fig. 1. A solenoid coil was used to generate magnetic field. Direct current was chosen for power supply so as to avoid inconvenient laminated structure of alternating current magnet. Electricity was transmitted in 220V alternating current to the self-locking device and converted to direct current by a bridge rectifier (not shown) locally. The coil was wound with enameled copper wire upon the coil framework. The framework was fitted on the tubular support and housed in the coil shell. A rubber mat was inserted between the framework and the coil shell in order to promote contact and improve thermal dissipation.

The lock plunger was connected with the ferromagnetic movable core. The movable core would be magnetically attracted by the stationary core and transmit the force to the lock plunger. The other end of the movable core was fixed with a signal pole, so that the plunger movement could be detected outside the guide sleeve. The stroke of the plunger was related with diameters of the cylinder and the piston pole. In our case the value is 8 mm.

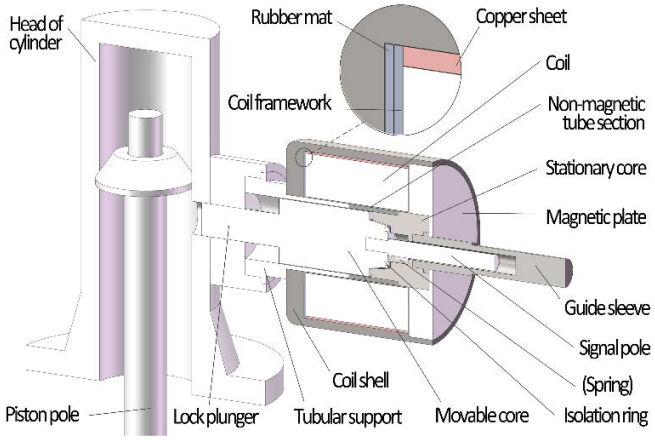

Fig.1 Typical structure of the self-locking device.

Beside the working air gap, the designed magnetic circuit was composed of tubular support, coil shell, magnetic plate, stationary core, and the movable core. These high-permeability parts guided magnetic flux around the designed path through the working gap [4].

Some positions of the device were expressly designed to modulate the magnet field. Although the tubular support was generally magnetic permeable, a section of it surrounding the working air gap was replaced by non-magnetic material. This non-magnetic tube section was used to restrain the magnetic line of force in the working air gap. Moreover, the corresponding faces of the movable core and the stationary core were inclined in design to adjust the relationship between attractive force and displacement of the movable core. Besides, an isolation ring was located at the end of movable core. When the movable core was attracted to the stationary core and the working air gap width was nominally diminished to 0, the isolation ring still separated the cores with a final minimum distance of 0.5 mm. therefore, the residual magnetic force could be reduced effectively at the beginning moment of a power cut.

STRUCTURAL OPTIMIZATION

The structural optimization of self-locking device with the aid of simulation was carried out in two steps. First, attractive force characteristic was analyzed by magnetic simulation with key geometric parameters of varied values. A set of optimized parameters were proposed. Second, the temperature rise of the as-optimized structure was verified with thermal analysis.

Magnetic analysis

Magnetostatic field analysis was performed on the self-locking device while time varying effects were ignored. The Difference Scalar Potential (DSP) method was applied in particular [5-6]. The device was reasonably simplified into a quarter-symmetric 3-D model without the cylinder since it was non-magnetic. The element Sourc36 was used to represent the

current distribution in the electromagnetic coil. The 3-D 10-node tetrahedral element Solid98, with scalar magnetic potential as the single degree of freedom, was employed to mesh the whole body of self-locking device. Additionally, the open boundary of surrounding air was covered by a layer of Infin111 elements to deal with the effect of magnetic far-field decay [7]. A typical meshed quarter-symmetric model is presented in Fig. 2. The solution was carried out with a convergence tolerance of 0.001 for both magnetic flux and magnetic potential. The calculated magnetic flux density was shown in Fig. 3.

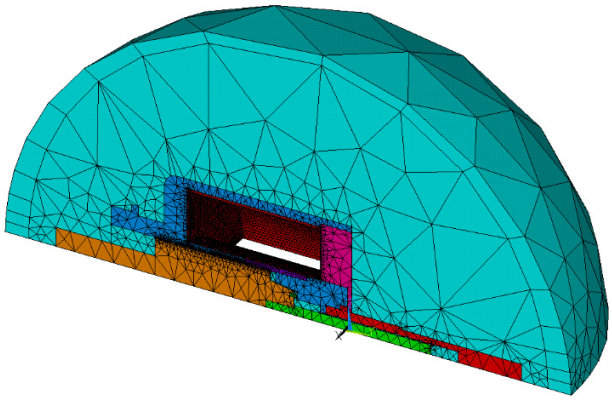

Fig.2 Meshed quarter-symmetric model for magnetic analysis with 0.5 mm working air gap (coil not shown).

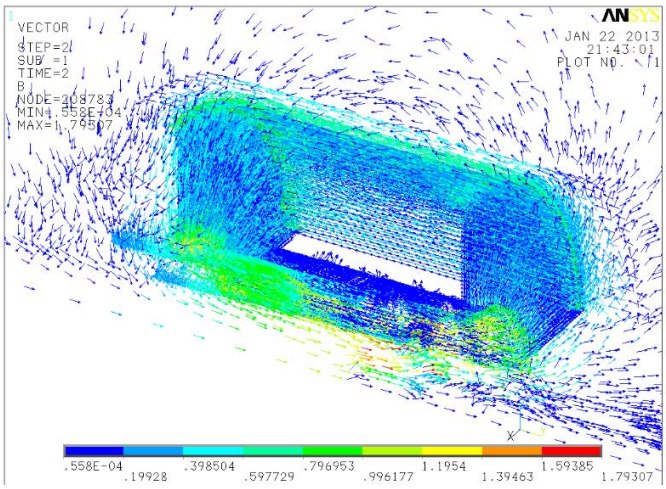

Fig. 3 Vector plot of magnetic flux density with 0.5 mm working air gap.

Effect of core face angle

For parallel board magnetic field, as is known to all, magnetic force is inversely proportional to the square of board distance. In the self-locking device, if the corresponding faces of the movable core and the stationary core were nearly perpendicular to the moving direction, the attractive force would change sharply when the core distance was small. The beginning attraction would be weak at the widest air gap. This attractive force characteristic would put the device at a disadvantage of likely unlocking failure. Therefore the corresponding faces of the cores should be inclined in design. The static electromagnetic attractive force between the cores with different corresponding face angles was calculated and compared. Simulation result of attractive force versus working air gap width with different core face angles was illustrated in Fig. 4. With the core structure of 28° inclination, the attractive force still increased significantly with the reduction of air gap width. While the angle was reduced to 10°, the attractive force curve was flatter in general than former case. A small platform even appeared in the curve with air gap between 2.5~5.5 mm. Moreover, the initial attractive force grew by about 20 N at the widest air gap. Above all, core structure of 10° inclination was concluded to be optimal for the self-locking device. Smaller angle might give rise to difficulty in the layout of isolation ring, and the attractive force would be reduced overmuch.

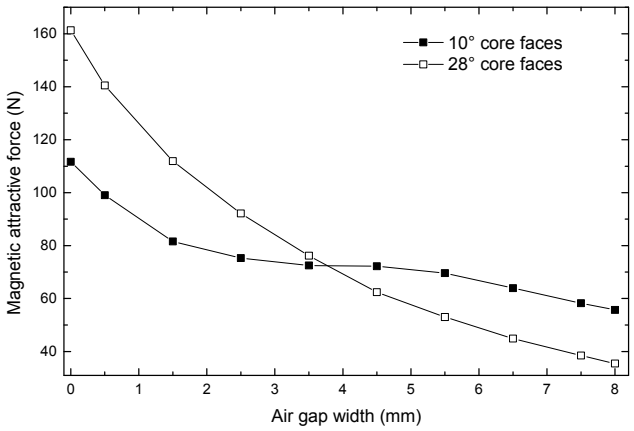

Fig. 4 Plot of calculated magnetic attractive force versus working air gap width with different core face angles.

Effect of non-magnetic tube section

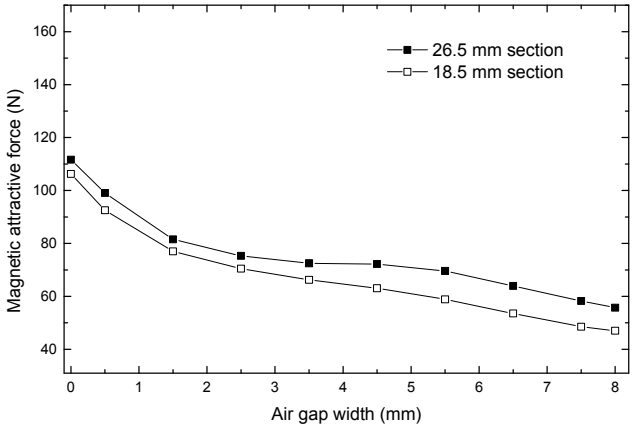

Fig. 5 Plot of calculated magnetic attractive force versus working air gap width with different non-magnetic tube section lengths.

An austenitic stainless steel tube section was welded on the end of tubular support near the working air gap. The relationship between magnetic force and the displacement with different lengths of non-magnetic tube section was demonstrated in Fig.

5. The attraction was strengthened when the non-magnetic tube section was longer, especially when the air gap was wider than 4.5 mm. With this non-magnetic tube section, the magnetic flux in the working air gap coming out from the stationary core would be mostly directed to the magnetic movable core. This would contribute to elevating the attractive force. Only a limited fraction of magnetic flux would leak away into the tubular support in radial direction.

On the basis of the simulation analysis above, structure of the self-locking device was optimized with 10° inclined core faces and 26.5-mm-long non-magnetic tube section. Furthermore, a compressive spring with large spring constant was employed to ensure successful self-lock when power-off. Consequently, the resultant force could be derived, as plotted in Fig. 6. Moreover, the displacement-time relationship could be deduced, which would be compared with the experimental data in next section.

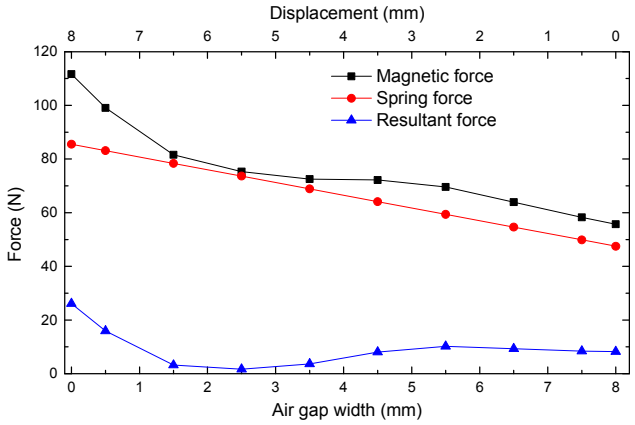

Fig. 6 Plot of calculated resultant force versus working air gap width.

Thermal analysis

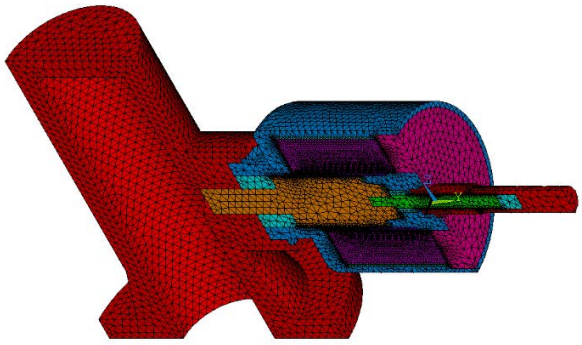

Fig.7 Meshed half-symmetric model for thermal analysis.

Transient thermal analysis [8] was carried out on the model of self-locking device in power-on state to verify that the temperature rise was affordable for the coil material. The initial and boundary conditions for the solution were: (a) the initial temperature was 298K according to actual environment; (b) the coil voltage was constant as 201VDC, while its current changed since the coil resistance increased with temperature; the initial value was 0.197A at 298K; (c) heat convection coefficient on the outer surfaces was 5 W/(m^2·K). An average heat generation rate was applied on the entire body of coil. The temperature varying effect of this rate, governed by the coil's electric resistance, was taken into account.

The 10-Node tetrahedral thermal solid element Solid87 was employed in the analysis. The half-symmetric 3-D model was meshed freely into 1.48 million elements (Fig. 7).

Steady-state temperature contour of the model was plotted in Fig. 8. The highest temperature was ~384 K inside the coil.

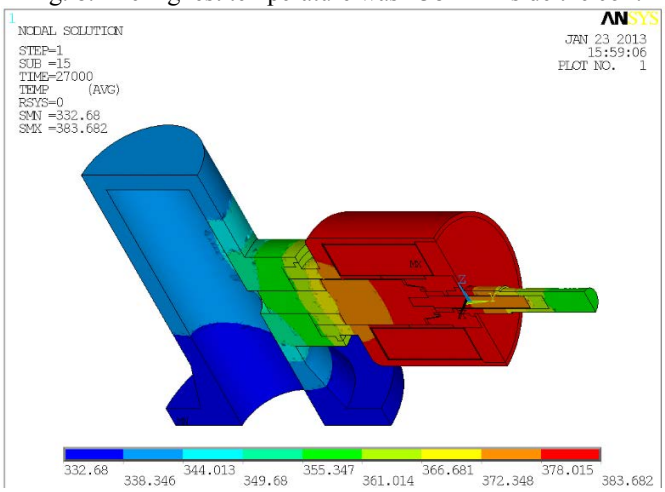

Fig. 8 steady-state temperature contour of the model.

PROTOTYPE TESTING RESULTS AND DISCUSSION

In order to verify the performance of the self-locking device practically, a prototype has been fabricated (Fig. 9(a)). In comparison with Fig. 1, a signal detecting unit was additionally installed outside the guide sleeve and housed by an austenitic stainless steel shell. A functional experiment was also conducted with a cylinder to validate the reliability of the prototype (Fig. 9(b)). The self-locking device worked properly with the cylinder for over 50 cycles of locking and unlocking.

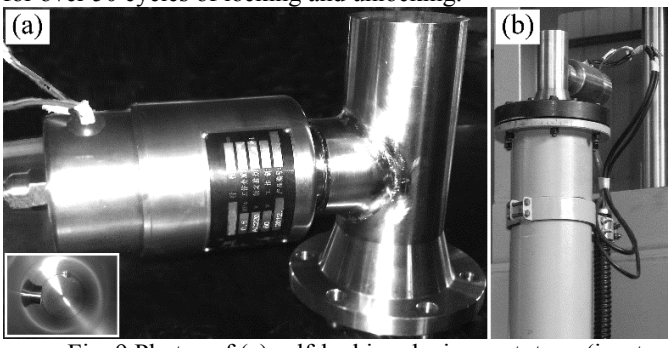

Fig. 9 Photos of (a) self-locking device prototype (inset: the lock plunger) and (b) its functional test with a vertical cylinder.

Plunger movement

The device was switched on and off to perform unlocking and locking actions. The movement of the plunger was shot by a high-speed camera and analyzed by image processing method.

Experimental displacement versus time data of unlocking process were plotted in Fig. 10. Meanwhile, the theoretical displacement curve was deduced from simulated resultant force data in Fig. 6 for comparison. The two curves showed good match from 0 to 0.02 s. After that the plunger was actually held momentarily for about 0.015 s before resuming movement. This was mainly due to the coil inductance elevation when the air gap getting narrow [9]. Further study is under way to calculate the dynamic behavior of the electromagnet by transient analysis method. Nevertheless, the calculated magnetostatic result still revealed that the design can provide sufficient attractive force sometime later, so that the locking and unlocking functions could be realized effectively, which was also verified by repeated test.

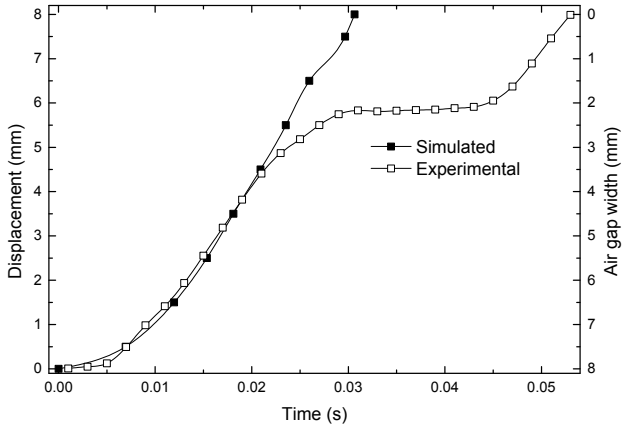

Fig. 10 Displacement versus time plot of unlocking process.

Temperature rise

The temperature rise test was performed at ambient temperature of 298 K. Only the coil temperature was measured via its electric resistance. The temperature rise curve of the coil in self-locking device was shown in Fig. 11. The temperature became steady at 380 K after about 30 min. This measured maximum temperature value was generally consistent with the simulation result (384 K). Accordingly, wire of thermal class 120 (E) or 130 (B) (IEC 62114) would be sufficient for the coil.

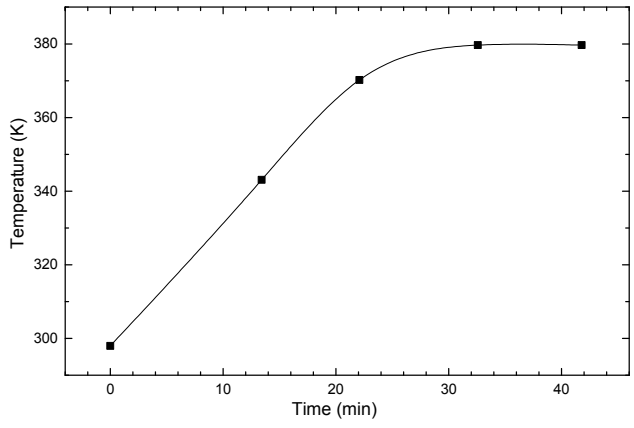

Fig. 11 Temperature rise curve of the coil in self-locking device.

CONCLUSIONS

A self-locking device was designed and fabricated for pneumatic cylinder in spent-fuel storage system of pebble-bed high temperature gas-cooled reactor.

The key structural parameters of the device, such as core face angle and non-magnetic section length, were optimized by finite element simulation. The theoretical estimation and experimental characterization has been carried out for the plunger movement. The temperature rise characteristic of the coil in the device was also calculated by finite element analysis and verified by experimental test.

Experimental result indicated that the device by optimized design could offer sufficient locking and unlocking forces and worked properly with the cylinder. The coil temperature rise was also affordable for practical use. The operating ambient temperature could reach 75℃ with wire of higher thermal class.

Similar self-locking devices for other pneumatic cylinders in radioactive environment of spent-fuel storage system could also be designed by the strategy presented in this work.

ACKNOWLEDGMENTS

This paper is supported by the National Science and Technology Major Project, Ministry of Science and Technology of China (Grant No. 2012ZX06901-021).

REFERENCES

1. **Nuclear Engineering and Design Vol. 239 No 7, 2009** - Current status and technical description of Chinese 2 × 250 MW_{th} HTR-PM demonstration plant, Zuoyi Zhang, et al
2. **Nuclear Engineering and Design Vol. 218 No 1–3, 2002** - The design features of the HTR-10, Zongxin Wu, Dengcai Lin, Daxin Zhong
3. **Nuclear Engineering and Design, Vol. 240 No 10, 2010** - Design and analysis of direct action solenoid valve based on computational intelligence, Qianfeng Liu, Hanliang Bo, Benke Qin
4. **Engineering Electromagnetics, 2003.** Kenneth R. Demarest
5. **Sensors and Actuators A: Physical Vol. 157, 2010** - Design, analysis and simulation of magnetostrictive actuator and its application to high dynamic servo valve, S. Karunanidhi, M. Singaperumal
6. **NDT&E International Vol. 39, 2006** - 3D FEM analysis in magnetic flux leakage method, Zuoying Huang, Peiwen Que, Liang Chen
7. **Fusion Engineering and Design Vol. 83 No 7–9, 2008** - Assessment of EM loads on the EU HCPB TBM during plasma disruption and normal operating scenario including the ferromagnetic effect, R. Roccella, et al
8. **Nuclear Fusion and Plasma Physics Vol. 31 No 2, 2011** - Thermodynamics performance study of cryostat feed of ITER correction coil system, Kai-song Wang, et al
9. **IEEE Transactions on Magnetics Vol. 41 No 3, 2005** - Modeling automotive gas-exchange solenoid valve actuators, Ryan R. Chladny, Charles Robert Koch, Alan F. Lynch